Dynamic Plastic Analysis of Impulsively Loaded Viscoplastic Rectangular Plates With Finite Deflections

David Hui
Department of Engineering Mechanics,
The Ohio State University,
Columbus, OH 43210

J. G. de Oliveira
Staff Engineer,
Conoco Inc.,
Houston, TX 77252

An energy balance method for the dynamic plastic analysis of thin rectangular plates made of a strain-rate sensitive material, taking into account the influence of finite-deflections, is proposed. The particular case of a fully clamped plate under uniformly distributed dynamic pressure pulse or blast loading is studied in some detail. In addition to the nonaxisymmetric and dynamic nature of the problem, the analysis considers important nonlinearities in the strains, equilibrium equations, and constitutive equations. Nonlinear ordinary differential equations in various regimes of plate deflections and loading histories are derived and solved using a Runge-Kutta method. Comparisons are made with existing experimental data.

1 Introduction

The effects of finite displacements and material strain-rate sensitivity on the dynamic behavior of rigid plastic structures are well known and have been extensively studied in the literature, as reviewed in detail by Jones (1975, 1978a, 1978b, 1979, 1981, 1985), Lee (1974), and Ari-Gur et al. (1984).

A simple beam model has been proposed by Perrone and Bhada (1979) and it was shown that this can lead to a practical method to account for plastic rate sensitivity with large deformations. This procedure has been successfully used in large deflections of viscoplastic circular membranes (Perrone and Bhadra, 1984). Mode approximation techniques, as discussed by Symonds and Wierzbicki (1979) and Symonds (1980), can be very powerful in dynamic plastic analysis since they can, in principle take into account material elasticity, strain hardening, and strain rate sensitivity effects, as well as geometry changes. However, no studies on rectangular plates using the above techniques have been reported.

For rectangular plates, studies have focused either on the rate insensitive materials with finite deflections (Jones, 1971) or strain-rate effects of the material with infinitesimal deflections (Wojewodzki and Wierzbicki, 1972). As indicated by Jones (1975), no theoretical studies appear to have been published on the dynamic response of rectangular plates when the influences of both finite displacements and material strain rate sensitivity are retained in the basic equations, even though such experimental data can be found in the literature. In the present paper, the approximate theoretical energy balance procedure proposed by Jones (1971) for the dynamic plastic behavior of rectangular plates with finite deflections will be extended to take material strain rate sensitivity effects into account.

A preliminary attempt was made by Taya and Mura (1974) to study the dynamic plastic behavior of strain rate sensitive rectangular plates with finite deflections. However, there is little theoretical basis to replace the dynamic yield stress by a factor times the corresponding static yield stress, and agreement with the experimental data is obtained by simple curve fitting. Later, Tuomala and Mikkola (1980) examined the same problem using the finite element method in conjunction with the Newmark scheme. They found that the viscoplastic analyis may considerably underestimate the experimentally reported permanent deflections of mild steel rectangular plates performed by Jones, Uran, and Tekin (1970), Further, it is not clear whether the discrepancies with experimental results are due to the various simplifying assumptions of the theoretical model or due to inaccuracies of the discretized scheme. Tuomala and Mikkola's conclusion that the viscoplastic analysis underestimates the experimental results needs to be confirmed by another independent method. In passing, Sureshwara et al. (1972) and Wu (1974) analyzed the dynamic plastic large deflections of clamped aluminum rectangular plates and reasonable agreement was found with the experiments conducted by Jones, Uran, and Tekin (1970) for aspect ratio 0.5926. Further experimental results on clamped rectangular plates with various aspect ratios were reported by Jones and Baeder (1972) and results on wide beams were presented by Jones and Van Duzer (1971). The analysis was extended to triangular pressure-time pulse by Jones (1973a).

In this case of mild steel rectangular plates, material strain rate sensitivity is known to have important effects on the response. As reported in the review paper by Jones (1975), the procedure of Jones (1971) was found to predict low but

Contributed by the Applied Mechanics Division for presentation at the Winter Annual Meeting, Anaheim, CA, December 7-12, 1986, of the American Society of Mechanical Engineers.

Discussion on this paper should be addressed to the Editorial Department, ASME, United Engineering Center, 345 East 47th Street, New York, N.Y., 10017, and will be accepted until two months after final publication of the paper itself in the JOURNAL OF APPLIED MECHANICS. Manuscript received by ASME Applied Mechanics Division, April 16, 1985; final revision March 18, 1986. Paper No. 86-WA/APM-34.

reasonable estimates of the maximum permanent lateral deflections for the mild steel rectangular plates tested by Jones, Uran, and Tekin (1970) and Jones and Baeder (1972). However, the estimates were obtained on the basis of some simplifications of the numerical procedure, so that the reported discrepancies with the experimental results cannot be attributed to the method itself. Thus, the authors present here an extension of the approximate theoretical energy balance procedure which takes material strain rate effects and finite deflections into consideration. This method of energy balance will be applied to the particular case of a mild steel clamped rectangular plate for which some experimental results are available, so that an assessment of its accuracy can be made. It appears that the feasibility of the application of the energy balance method to viscoplastic plates undergoing finite deflections has not been demonstrated in the open literature.

2 Constitutive and Basic Equations

Consider an initially, flat, rigid perfectly plastic plate of arbitrary shape, which deforms into a number of rigid regions separated by r time-independent straight line plastic hinges each of length C_m where $m=1, 2, \ldots r$. If in-plane deflections are negligible in comparison with the out-of-plane deflections, such as would be the case when attention is restricted to transverse loading, then it can be shown that the energy balance equation is (Jones, 1971)

$$\iint (p_3 - \mu W,_{\bar{t}\bar{t}}) W,_{\bar{t}} dA = \sum_{m=1}^{r} \int_{C_m} (NW - M)(\theta_{m,\bar{t}}) dC_m \tag{1}$$

The left side is the external work rate and the right side represents the total internal energy dissipation rate along all the plastic hinges in the plate. In the above equation, A is the total surface area of the plate, μ is the mass of the plate per unit surface area, $\bar{t}$ is time, $\theta_{m,\bar{t}}$ is the relative angular rotation rate across a straight line hinge and p_3 is the applied downward transverse pressure. The transverse displacement W is measured vertically downwards from the plate's middle surface and the transverse velocity and acceleration rare, respectively, $W,_{\bar{t}}$ and $W,_{\bar{t}\bar{t}}$. Further, N is the membrane force per unit length which is positive at a hinge when it produces stretching across the plate's thickness. Finally, M is the bending moment per unit length which is positive when the material on the upper surface of the plate is stretched. Note that the moment M and the rotation rate $\theta_{m,\bar{t}}$ should always have opposite signs.

As discussed in Jones (1971), it is convenient to define

$$D_h = (NW - M)(\theta_{m,\bar{t}}) \tag{2}$$

$$D_b = (-M)(\theta_{m,\bar{t}}) \tag{3}$$

where D_h and D_b are the internal energy dissipation rate per unit length at a straight line interior and boundary hinge, respectively. The explicit form of the hinge dissipation function depends on the type of supports around the boundary of the plate and on the yield condition for the material.

Strain rate sensitivity (or viscoplastic behavior) of the material can be taken into account by the well known empirical approximate Cowper–Symonds constitutive equation (Symonds, 1965),

$$\sigma(Z)/\sigma_o = 1 + [\epsilon(Z),_{\bar{t}}/D]^{1/n} \tag{4}$$

where $\sigma(Z)$ is the stress (which is a function of the out-of-plane coordinate Z measured from the plate middle surface, positive downwards), σ_o is the uniaxial tensile yield stress, $\epsilon(Z),_{\bar{t}}$ is the strain rate and both D and n are positive real material constants. Because of its simplicity, the above constitutive equation has been used successfully by a number of authors to solve a variety of dynamic problems (Jones, 1975) and is known to provide a reasonably good representative of uniaxial tests up to strain rates of 1000 s^{-1}. For hot rolled mild steel, the values $D=40.4$ s^{-1} and $n=5$ have proved to be quite satisfactory.

As suggested in Symonds and Jones (1972), the above constitutive equation can be used to derive the dynamic plastic bending moment and axial force for strain rate sensitive behavior. It can be useful to write it in the more general form

$$\sigma(Z)/\sigma_o = a + (b)[\epsilon(Z),_{\bar{t}}/D]^{1/n} \tag{5}$$

where a and b are dimensionless coefficients (not to be confused with the length and width of the plate). Thus, $a=1$, $b=0$ corresponds to the rigid-plastic analysis, while $a=b=1$ corresponds to the Cowper–Symonds equation. For large n the stress increases rapidly at very small strain rates, but for strain rate above, say, 10 s^{-1}, the curve is very flat. Thus, convenient linearizations of the constitutive equation can be obtained by making $n=1$ and adjusting the values of a and b. In particular, for $a=0$ and $n=1$, a homogeneous relation can be obtained which has proved to be quite powerful (Wojno and Wierzbicki, 1979).

Following the approach suggested by Jones (1973b), consider a clamped span of length $2L$ which remains entirely rigid except at hinges which develop at the center and the supports. The axial extension of the mid-surface is

$$2(L^2 + W^2)^{1/2} - 2L \simeq W^2/L \tag{6}$$

where W is the transverse deflection at the central hinge. Assuming that the width of the hinge at each support is l (note that l is usually of the order of the plate thickness for small deflections), the width of the central hinge is $2l$, and the axial extension is shared equally by these three plastic hinges, then the axial strain and the corresponding axial strain rate are

$$\epsilon = W^2/(4lL), \quad \epsilon,_{\bar{t}} = (W)(W,_{\bar{t}})/(2lL) \tag{7}$$

Similarly, the curvature change at each hinge and the curvature rate are

$$\kappa = W/(lL), \quad \kappa,_{\bar{t}} = (W,_{\bar{t}})/(lL) \tag{8}$$

Thus,

$$\epsilon,_{\bar{t}}/\kappa,_{\bar{t}} = W/2 \tag{9}$$

and if plane cross sections remain plane during deformation or

$$\epsilon,_{\bar{t}} = (e)(\kappa,_{\bar{t}}) \tag{10}$$

one obtains (H is the plate thickness)

$$2e/H = W/H = w \tag{11}$$

The dynamic plastic bending moment per unit length, M, can now be obtained by integrating the product $Z\sigma(Z)$ across the plate thickness (from $Z=-H/2$ to $Z=-e$ and from $Z=-e$ to $Z=H/2$ for small deflections $W \le H$ and from $Z=-H/2$ to $Z=H/2$ for the large deflection regime $W>H$, see Fig. 1(a), 1(b)) and the stress, being a function of Z, is given by equation (5). Similarly, the dynamic axial force per unit length, N, is given by the integral of $\sigma(Z)$ across the plate thickness. In performing these integrations, it should be noted that the strain rate as a function of Z is related to the curvature rate $\kappa,_{\bar{t}}$ (where $\kappa,_{\bar{t}}$ is independent of Z) by

$$\epsilon(Z),_{\bar{t}} = (Z+e)(\kappa,_{\bar{t}}) \tag{12}$$

as shown in Fig. 1. Note that e is the instantaneous distance of the center of rotation above the plate's middle surface. Using these definitions, the following results can be obtained for M and N for the small deflection regime $e \le H/2$ (where $w = W/H = 2e/H$):

$$M/M_o = (a)(1-w^2) + (b)\left(\frac{\kappa,_{\bar{t}}H}{2D}\right)^{1/n} \left\{ [(1+w)^{2+(1/n)} + (1-w)^{2+(1/n)}]\left(\frac{n}{1+2n} - \frac{n}{1+n}\right) + [(1+w)^{1+(1/n)} + (1-w)^{1+(1/n)}]\left(\frac{n}{1+n}\right) \right\} \tag{13}$$

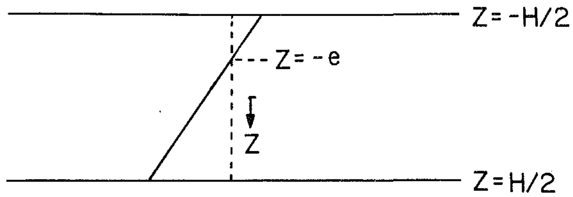

Fig. 1(a) Stress distribution over the plate thickness in the small deflection regime

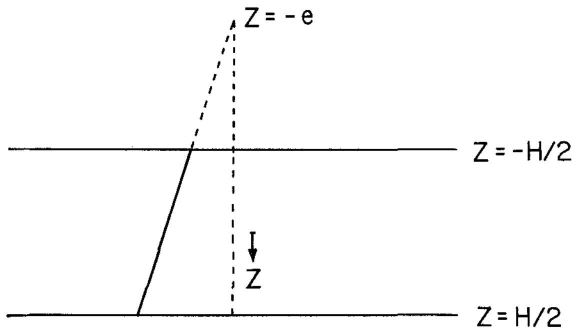

Fig. 1(b) Stress distribution over the plate thickness in the large deflection regime

$$N/N_o=(a)(w)+\left(\frac{bn}{2(1+n)}\right)\left(\frac{\kappa_{,\bar{t}}H}{2D}\right)^{1/n}\{(1+w)^{1+(1/n)}-(1-w)^{1+(1/n)}\} \quad (14)$$

For the large deflection regime $e \geq H/2$, one obtains

$$M/M_o=(b)\left(\frac{H\kappa_{,\bar{t}}}{2D}\right)^{1/n}\Big\{[(w+1)^{2+(1/n)}-(w-1)^{2+(1/n)}]\left(\frac{n}{1+2n}-\frac{n}{1+n}\right)+[(w+1)^{1+(1/n)}+(w-1)^{1+(1/n)}]\left(\frac{n}{n+1}\right)\Big\} \quad (15)$$

$$N/N_o=a+\left(\frac{bn}{2(1+n)}\right)\left(\frac{\kappa_{,\bar{t}}H}{2D}\right)^{1/n}\{(w+1)^{1+(1/n)}-(w-1)^{1+(1/n)}\} \quad (16)$$

In the above, M_o is the static fully plastic bending moment per unit length ($M_o=\sigma_o H^2/4$) and N_o is the static fully plastic membrane force per unit length ($N_o=\sigma_o H$). In the present analysis, the exact forms for M/M_o and N/N_o are retained without the use of the binomial approximation employed by Symonds and Jones (1972). Thus, for the small deflection regime ($w \leq 1$), the dissipation function for the interior hinge D_h takes the form

$$\frac{D_h}{M_o|\theta_{m,\bar{t}}|}=(a)(1+3w^2)+(b)\left(\frac{\kappa_{,\bar{t}}H}{2D}\right)^{1/n}\Big\{\left(\frac{n}{1+n}+\frac{n}{1+2n}\right)[(1+w)^{2+(1/n)}+(1-w)^{2+(1/n)}]-\left(\frac{n}{1+n}\right)[(1+w)^{1+(1/n)}+(1-w)^{1+(1/n)}]\Big\} \quad (17)$$

while the dissipation function for the large deflection regime ($w \geq 1$) becomes

$$\frac{D_h}{M_o|\theta_{m,\bar{t}}|}=(4a)(w)+(b)\left(\frac{\kappa_{,\bar{t}}H}{2D}\right)^{1/n}\Big\{[(w+1)^{2+(1/n)}-(w-1)^{2+(1/n)}]\left(\frac{n}{1+n}+\frac{n}{1+2n}\right)+[(w+1)^{1+(1/n)}+(w-1)^{1+(1/n)}]\left(\frac{-n}{1+n}\right)\Big\} \quad (18)$$

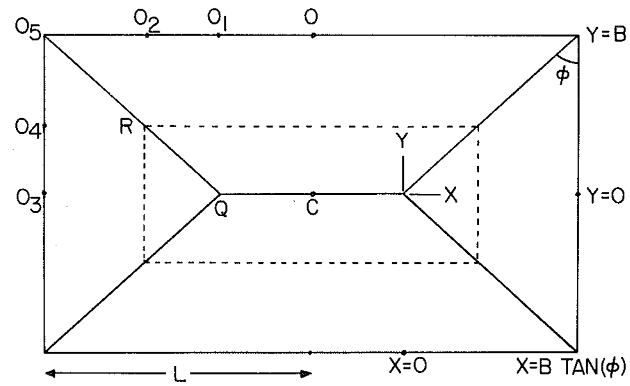

Fig. 2 Deflection profile of a clamped rectangular plate under impulsive load

Finally, the dissipation function for the hinges that form around the clamped boundary of a rectangular plate is given by

$$\frac{D_b}{M_o|\theta_{m,\bar{t}}|}=|M|/M_o \quad (19)$$

where M/M_o is given by equation (13) or (15) for the small and large deflection regimes, respectively, and w denotes the nondimensional displacement at the interior hinge corresponding to the boundary hinge. Note that equations (11) and (19) apply to the case where the rectangular plate is clamped all around. For other types of support conditions, equivalent expressions have to be derived. It is clear from the derivation of the dissipation functions that the expressions for D_h and D_b can only be used to sum up the total energy dissipation in a given plate and for a given set of boundary conditions. Thus, they cannot be used independently to give the energy dissipation at a particular hinge, but only for the plate as a whole. Thus, the energy dissipation at a particular hinge used in the subsequent analysis is used for mathematical convenience only. When $a=1$ and $b=0$, the rigid plastic solution must be recovered, and it can easily be shown that the dissipation functions D_h and D_b reduce to the corresponding equations derived by Jones and Walters (1971).

The subsequent analysis deals with a thin, rigid perfectly plastic rectangular plate of length $2L$ and width $2B$ which is fully clamped around the outer boundary as indicated in Fig. 2. The plate is subjected to a uniformly distributed dynamic load with the following pressure time history:

$$p_3(\text{at } 0 \leq \bar{t} \leq \bar{t}_1)=p_o, \quad p_3(\text{at } \bar{t} > \bar{t}_1)=0 \quad (20)$$

where $\bar{t}_1$ is the duration of the pressure pulse. It is assumed here that the shape of the displacement field for the dynamic case is the same as the velocity profile used by Wood (1961) to give an upper bound to the collapse load of the corresponding static problem. Using the roof-shape deformation pattern, the displacement at the interior inclined hinge can be written in the form

$$w=(1-y)w_c \quad (21)$$

where $w_c=W_c/H$, W_c is the deflection at the center of the rectangular plate, $y=Y/B$ and Y ranges from 0 to B (see Fig. 2).

In the dynamic analysis that follows, it is necessary to consider the two loading conditions specified by equations (20). In both cases, the two possibilities $w_c \leq 1$ and $w_c > 1$ have to be taken into account.

3 Differential Equation in the Small Deflection Regime ($w_c \leq 1$)

If equations (20) and (21) are substituted into the left side of the energy balance equation (1), making use of $X = Y\tan\phi$ (see Fig. 2) and integrating over the four regions in the roof-shaped deformation pattern, the following result can be obtained (see Jones, 1971):

$$\frac{\text{left side}}{M_o W_{c,\bar{t}}} = L_1 + L_2 w_{c,tt} \tag{22}$$

where

$$L_1 = (2\eta/3)(L/B)\left(\frac{12(3-\xi_o)}{3-2\xi_o}\right), \tag{23a}$$

$$L_2 = (2/3)(L/B)(B^2 H\mu D^2/M_o)(-2+\xi_o) \tag{23b}$$

$$t = \bar{t}D, \tag{23c}$$

$$\eta = p_o/p_c, \tag{23d}$$

$$p_c = 12M_o/[B^2(3-2\xi_o)], \tag{23e}$$

$$\xi_o = (B/L)\tan\phi \tag{23f}$$

$$\tan\phi = -(B/L) + [3+(B/L)^2]^{1/2} \tag{23g}$$

Note that p_c is the magnitude of the static collapse pressure and the value of ϕ ranges from 45 deg for a square plate ($L/B = 1$) to 60 deg for an infinitely long plate ($L/B = \infty$). As suggested by Jones (1971), for moderate values of permanent deflections, the static collapse velocity profile is a reasonable choice for the displacement field in the corresponding dynamic problem to ensure the smallest upper bound to the static collapse pressure.

The right side of the energy balance equation (1) can be written as the sum of the energy dissipation along (see Fig. 2)

(*i*) the interior inclined hinges, $4E[QO_5]$
(*ii*) the interior central hinge, $2E[CQ]$
(*iii*) the boundary hinges parallel to the X axis, $4E[OO_5]$
(*iv*) the boundary hinges parallel to the Y axis, $4E[O_3O_5]$

where, for example, $E[QO_5]$ is the energy dissipation along the hinge from Q to O_5 (see Fig. 2).

Along the interior inclinded hinges, the dissipation function is given by equation (17), $w = (1-y)w_c$, and the rotation rate and the curvature rate are given by

$$\theta,_{\bar{t}} = W_{c,\bar{t}}/(B\sin\phi), \quad \kappa,_{\bar{t}} = W_{c,\bar{t}}/(2lB\sin\phi) \tag{25}$$

where $2l$ is the hinge width. Thus, it can be shown that the energy dissipated along these hinges is

$$\frac{4E[QO_5]}{M_o W_{c,\bar{t}}} = \left(\frac{4}{\sin\phi\cos\phi}\right)\left\{(a)(1+w_c^2) + b\left(\frac{w_{c,t}}{4h^*\sin\phi}\right)^{1/n}\right.$$
$$\left.\left[\left(\frac{n}{1+n}+\frac{n}{1+2n}\right)G_2(w_c) - \left(\frac{n}{n+1}\right)G_1(w_c)\right]\right\} \tag{26}$$

where $h^* = Bl/H^2$ and

$$G_1(w_c) = [n/(1+2n)](1/w_c)[(1+w_c)^{2+(1/n)} - (1-w_c)^{2+(1/n)}]$$
$$G_2(w_c) = [n/(1+3n)](1/w_c)[(1+w_c)^{3+(1/n)} - (1-w_c)^{3+(1/n)}] \tag{27}$$

Similarly, along the interior central hinges, the dissipation function is again given by equation (17), but with $w = w_c$. The rotation rate and the curvature rate are

$$\theta,_{\bar{t}} = 2W_{c,\bar{t}}/B, \quad \kappa,_{\bar{t}} = W_{c,\bar{t}}/(Bl) \tag{28}$$

so that the following expression can be obtained:

$$\frac{2E[CQ]}{M_o W_{c,\bar{t}}} = (4)[(L/B)-\tan\phi]\left\{(a)(1+3w_c^2) + (b)\left(\frac{w_{c,t}}{2h^*}\right)^{1/n}\right.$$
$$\left(\left(\frac{n}{1+n}+\frac{n}{1+2n}\right)[(1+w_c)^{2+(1/n)} + (1-w_c)^{2+(1/n)}]\right.$$
$$\left.\left.-\left(\frac{n}{1+n}\right)[(1+w_c)^{1+(1/n)} + (1-w_c)^{1+(1/n)}]\right)\right\} \tag{29}$$

The boundary hinges parallel to the X axis can be obtained in a similar way, but now the dissipation function is given by equation (19). Since W denotes the displacement at the interior hinge corresponding to the boundary hinge, the integration has to be computed in two intervals. In the interval OO_1 (see Fig. 2), the displacement is uniform and $w = w_c$, while in the interval O_1O_5, it is given by $w = (1-y)w_c$. Along the boundary hinges OO_1 and O_1O_5, the rotation rate and the curvature rate are

$$\theta,_{\bar{t}} = W_{c,\bar{t}}/B, \quad \kappa,_{\bar{t}} = W_{c,\bar{t}}/(Bl) \tag{30}$$

so that one obtains

$$\frac{(4)(E[OO_1]+E[O_1O_5])}{M_o W_{c,\bar{t}}}$$
$$= (a)(4L/B)\{1+(w_c^2)[-1+(2/3)(B/L)\tan\phi]\}$$
$$+(4b)\left(\frac{w_{c,t}}{2h^*}\right)^{1/n}\left\{[(L/B)-\tan\phi]\left(\left(\frac{n}{1+2n}\right.\right.\right.$$
$$\left.+\frac{n}{1+n}\right)[(1+w_c)^{2+(1/n)} + (1-w_c)^{2+(1/n)}]$$
$$\left.+\left(\frac{n}{1+n}\right)[(1+w_c)^{1+(1/n)} + (1-w_c)^{1+(1/n)}]\right)$$
$$\left.+(\tan\phi)\left[\left(\frac{n}{1+2n}-\frac{n}{1+n}\right)G_2(w_c) + \left(\frac{n}{1+n}\right)G_1(w_c)\right]\right\} \tag{31}$$

Finally, the rotation rate and the curvature rate for the boundary hinges parallel to the Y axis are

$$\theta,_{\bar{t}} = W_{c,\bar{t}}/(B\tan\phi), \quad \kappa,_{\bar{t}} = W_{c,\bar{t}}/(Bl\tan\phi) \tag{32}$$

so that

$$\frac{4E[O_3O_5]}{M_o W_{c,\bar{t}}} = (a)(4/\tan\phi)[1-(1/3)(w_c^2)]$$
$$+(b)(4/\tan\phi)\left(\frac{W_{c,t}}{2h^*\tan\phi}\right)^{1/n}$$
$$\left\{\left(\frac{n}{1+2n}-\frac{n}{1+n}\right)G_2(w_c) + \left(\frac{n}{1+n}\right)G_1(w_c)\right\} \tag{33}$$

Assembling all the above expressions, the energy balance equation (1) can be written in the form of a nonlinear ordinary differential equation ($w_c \le 1$):

$$L_1 + L_2 w_{c,tt} = (a)(c_3 + c_4 w_c^2) + (b)[w_{c,t}/(2h^*)]^{1/n}$$
$$[c_oG_o(w_c) + c_1G_1(w_c) + c_2G_2(w_c)] \tag{34}$$

where

$$c_o = (4)\left(\frac{2n}{1+2n}\right)[(L/B)-\tan\phi] \tag{35a}$$

$$c_1 = (4)\left(\frac{n}{1+n}\right)\left[\left(\frac{-1}{\sin\phi\cos\phi}\right)\left(\frac{1}{2\sin\phi}\right)^{1/n}\right.$$
$$\left.+\tan\phi + (1/\tan\phi)^{1+(1/n)}\right] \tag{35b}$$

$$c_2 = (4)\left\{\left(\frac{n}{1+n}+\frac{n}{1+2n}\right)\left(\frac{1}{\sin\phi\cos\phi}\right)\left(\frac{1}{2\sin\phi}\right)^{1/n}\right.$$
$$\left.+\left(\frac{n}{1+2n}-\frac{n}{1+n}\right)[\tan\phi + (1/\tan\phi)^{1+(1/n)}]\right\} \tag{35c}$$

$$c_3 = (4)\left[\left(\frac{1}{\sin\phi\cos\phi}\right) + (2L/B) - \tan\phi + (1/\tan\phi)\right] \tag{35d}$$

$$c_4 = (4)\left\{\left(\frac{1}{\sin\phi\cos\phi}\right) + (2L/B)\right.$$
$$\left.-(7/3)\tan\phi - (1/3)(1/\tan\phi)\right\} \tag{35e}$$

$$G_o(w_c) = (1+w_c)^{2+(1/n)} + (1-w_c)^{2+(1/n)} \tag{35f}$$

Based on a static analysis (Jones and Walters, 1971), the angle ϕ is related to the aspect ratio B/L by equation (23g) which implies,

$$\tan^2(\phi) = 3-2\xi_o, \quad (36a)$$

$$\sin^2(\phi) = (3-2\xi_o)/(4-2\xi_o) \quad (36b)$$

Using these relations, the coefficients of the above differential equation degenerate to these presented by Jones (1971) for the strain-rate insensitive case.

In the special case of aspect ratio being 0.59259 (Jones, Uran, and Tekin, 1970) and $n=5$, one obtains ($\tan\phi = 1.2380$, $\xi_o = 0.73364$)

$$L_1 = 19.9618\,\eta, \quad (36c)$$

$$L_2 = -1.424649(B^2 H \mu D^2/M_o) \quad (36d)$$

$$c_o = 1.634449, \quad (36e)$$

$$c_1 = 0.464410, \quad (36f)$$

$$c_2 = 6.598625, \quad (36g)$$

$$c_3 = 19.961898, \quad (36h)$$

$$c_4 = 9.051158 \quad (36i)$$

4 Differential Equation in the Large Deflection Regime ($w_c > 1$)

If the deflection at the center of the rectangular plate is greater than one, the internal energy dissipation rate is governed by equation (18) in those portions of the hinge lines (near the center) which have deflections greater than the plate thickness. For the remainder of the plate (away from the center) the dissipation function for the small deflection regime can be obtained from equation (17). Thus, as w_c increases beyond 1, a time-dependent rectangular shaped boundary travels outwards from the central line hinge towards the plate's edges. This boundary always has a deflection $w=1$ and it divides the plate into two regions: an outer zone which has $w<1$ and an inner zone with $w>1$.

Following the same approach as used in the last section, it can be shown that the energy dissipations along the interior inclined hinges are (see Fig. 2)

$$\frac{4E[QR]}{M_o W_{c,\bar{t}}} = \left(\frac{4}{\sin\phi\cos\phi}\right)\Big\{(2a)[w_c-(1/w_c)]+(b)\left(\frac{w_{c,t}}{4h^*\sin\phi}\right)^{1/n}\Big[\left(\frac{n}{1+n}+\frac{n}{1+2n}\right)G_4(w_c) - \left(\frac{n}{1+n}\right)G_3(w_c)\Big]\Big\} \quad (37a)$$

$$\frac{4E[RO_5]}{M_o W_{c,\bar{t}}} = \left(\frac{4}{\sin\phi\cos\phi}\right)\Big\{(2a/w_c)+(b)\left(\frac{w_{c,t}}{4h^*\sin\phi}\right)^{1/n}\Big[\left(\frac{n}{1+n}+\frac{n}{1+2n}\right)G_6(w_c)-\left(\frac{n}{1+n}\right)G_5(w_c)\Big]\Big\} \quad (37b)$$

where

$$G_3(w_c) = \left(\frac{-n}{1+2n}\right)\left(\frac{1}{w_c}\right)\{2^{2+(1/n)}-(w_c+1)^{2+(1/n)} - (w_c-1)^{2+(1/n)}\} \quad (38a)$$

$$G_4(w_c) = \left(\frac{-n}{1+3n}\right)\left(\frac{1}{w_c}\right)\{2^{3+(1/n)}-(w_c+1)^{3+(1/n)} + (w_c-1)^{3+(1/n)}\} \quad (38b)$$

$$G_5(w_c) = [n/(1+2n)](1/w_c)[2^{2+(1/n)}] \quad (38c)$$

$$G_6(w_c) = [n/(1+3n)](1/w_c)[2^{3+(1/n)}] \quad (38d)$$

The energy dissipation at the interior central hinge is

$$\frac{2E[CQ]}{M_o W_{c,\bar{t}}} = (4)[(L/B)-\tan\phi]\Big\{(a)(4w_c)+(b)\left(\frac{w_{c,t}}{2h^*}\right)^{1/n}\Big(\left(\frac{n}{1+n}+\frac{n}{1+2n}\right)[(w_c+1)^{2+(1/n)}-(w_c-1)^{2+(1/n)}] - \left(\frac{n}{1+n}\right)[(w_c+1)^{1+(1/n)}+(w_c-1)^{1+(1/n)}]\Big)\Big\} \quad (39)$$

Regarding now the boundary hinges, as happens with the interior inclined hinges, it is necessary to make a distinction between those portions of the hinges where the corresponding internal hinges are in the large deflection profile, and those portions which are governed by the small deflection equations. Thus, one obtains the energy dissipation at the boundary hinges parallel to the X axis:

$$\frac{4E[O_2O_5]}{M_o W_{c,\bar{t}}} = 4\tan\phi\Big\{(a)\left(\frac{2}{3w_c}\right)+(b)\left(\frac{w_{c,t}}{2h^*}\right)^{1/n}\Big[\left(\frac{n}{1+2n}-\frac{n}{1+n}\right)G_6(w_c)+\left(\frac{n}{1+n}\right)G_5(w_c)\Big]\Big\} \quad (40)$$

$$\frac{4E[O_1O_2]}{M_o W_{c,\bar{t}}} = (4\tan\phi)(b)\left(\frac{w_{c,t}}{2h^*}\right)^{1/n}\Big\{\left(\frac{n}{1+2n}-\frac{n}{1+n}\right)G_4(w_c)+\left(\frac{n}{1+n}\right)G_3(w_c)\Big\} \quad (41)$$

$$\frac{4E[OO_1]}{M_o W_{c,\bar{t}}} = (4)[(L/B)-\tan\phi](b)\left(\frac{w_{c,t}}{2h^*}\right)^{1/n}\Big[\left(\frac{n}{1+2n}-\frac{n}{1+n}\right)[(w_c+1)^{2+(1/n)}-(w_c-1)^{2+(1/n)}] + \left(\frac{n}{1+n}\right)[(w_c+1)^{1+(1/n)}+(w_c-1)^{1+(1/n)}]\Big] \quad (42)$$

Finally, the energy dissipations along the hinges parallel to the Y axis are

$$\frac{4E[O_4O_5]}{M_o W_{c,\bar{t}}} = \left(\frac{4}{\tan\phi}\right)\Big\{(a)\left(\frac{2}{3w_c}\right)+b\left(\frac{w_{c,t}}{2h^*\tan\phi}\right)^{1/n}\Big[\left(\frac{n}{1+2n}-\frac{n}{1+n}\right)G_6(w_c)+\left(\frac{n}{1+n}\right)G_5(w_c)\Big]\Big\} \quad (43)$$

$$\frac{4E[O_3O_4]}{M_o W_{c,\bar{t}}} = \left(\frac{4}{\tan\phi}\right)(b)\left(\frac{w_{c,t}}{2h^*\tan\phi}\right)^{1/n}\Big\{\left(\frac{n}{1+2n}-\frac{n}{1+n}\right)G_4(w_c)+\left(\frac{n}{1+n}\right)G_3(w_c)\Big\} \quad (44)$$

Assembling the above results, the energy balance equation (for the case when the deflection at the center of the rectangular plate w_c exceeds one) can be written in the form of a nonlinear ordinary differential equation in the form,

$$L_1 + L_2 w_{c,tt} = (a)[d_3 w_c + (d_4/w_c)] + (b)\left(\frac{w_{c,t}}{2h^*}\right)^{1/n}\{[(w_c+1)^{2+(1/n)}-(w_c-1)^{2+(1/n)}][d_o+(d_1/w_c)] + (d_2)[(w_c+1)^{3+(1/n)}-(w_c-1)^{3+(1/n)}](1/w_c)\} \quad (45)$$

where

$$d_o = [(L/B)-\tan\phi](8n)/(1+2n) \quad (46a)$$

$$d_1 = \left[\tan\phi+\left(\frac{1}{\tan\phi}\right)^{1+(1/n)} - \left(\frac{1}{2\sin\phi}\right)^{1/n}\left(\frac{1}{\sin\phi\cos\phi}\right)\right]\left(\frac{4n^2}{(1+n)(1+2n)}\right) \quad (46b)$$

$$d_2 = \left[\left(\frac{1}{2\sin\phi}\right)^{1/n}\left(\frac{1}{\sin\phi\cos\phi}\right)\left(\frac{n}{1+n}+\frac{n}{1+2n}\right)\right.$$
$$+\left[\tan\phi+\left(\frac{1}{\tan\phi}\right)^{1+(1/n)}\right] \quad (46c)$$
$$\left.\cdot\left(\frac{n}{1+2n}-\frac{n}{1+n}\right)\right]\left(\frac{4n}{1+3n}\right)$$

$$d_3 = \left(\frac{8}{\sin\phi\cos\phi}\right)+16[(L/B)-\tan\phi] \quad (46d)$$

$$d_4 = \frac{8}{3\sin\phi\cos\phi} \quad (46e)$$

In the special case of $B/L = 0.5925925$ and $n = 5$ examined by Jones–Uran–Tekin (1970), one obtains

$$d_o = 1.63444, \quad (47a)$$
$$d_1 = 0.21109, \quad (47b)$$
$$d_2 = 2.06207, \quad (47c)$$
$$d_3 = 23.5576, \quad (47d)$$
$$d_4 = 5.45537 \quad (47e)$$

As a check on the analysis, it can be shown that the foregoing ordinary differential equations for the small and large deflection regimes agree in the special case when $w_c = 1$. As expected, it is found that when $a = 1$ and $b = 0$, the foregoing two ordinary differential equations agree with that obtained by Jones (1971) for a rigid-plastic rectangular plate. If, in addition to setting $a = 1$, $b = 0$, the inertia term $w_{c,tt}$ is made zero, the ordinary differential equations for the small and large deflection regime yield the load deflection relationship derived by Jones and Walters (1971) for a fully clamped rectangular plate subjected to a uniform static transverse pressure.

The dynamic plastic plate response can be obtained following a method similar to the one outlined by Jones (1971). It is expected that for an impulsive load, the maximum permanent deflection for $\eta = p_o/p_c = 100$ and $\eta =$ infinity essentially coincide. The initial conditions are

$$w(t=0)=0$$
$$w_{,t}(t=0)=0 \quad (48)$$

In order to ensure that the initial momentum matches the external impulse, it is necessary to set

$$p_o\bar{t}_1 = \mu V_o \quad (49a)$$

where $V_o = W_{,t}(t=0)$ is the initial velocity. Thus, the nondimensional duration of the pressure pulse is $t_1 = \mu V_o D/(\eta p_c)$, so that

$$\eta = 100 \text{ for } t \le t_1, \quad \eta = 0 \text{ for } t > t_1 \quad (49b)$$

In the above, $t_1 = \bar{t}_1 D$, $p_o = \eta p_c$ and the values $D = 40.4\ \text{s}^{-1}$, $n = 5$ are chosen for mild steel plates in the Cowper–Symonds constitutive equation.

The nonlinear ordinary differential equations for the small and large deflection regimes are solved here numerically on the basis of Runge–Kutta formulae of order five and six (Hull et al., 1976) with sufficiently small tolerance. The time step is chosen sufficiently small to ensure convergence and to make possible an accurate definition of the transition between the various phases of motion, as well as an accurate determination of the maximum permanent deflection. Approximately 21 time steps are chosen between $t = 0$ and $t = 0.999t_1$. The numerical procedure is applied to the three stages of motion defined by Jones (1971).

5 Discussion of Results

In order to assess the accuracy of the present energy balance method in predicting the response of impulsively loaded

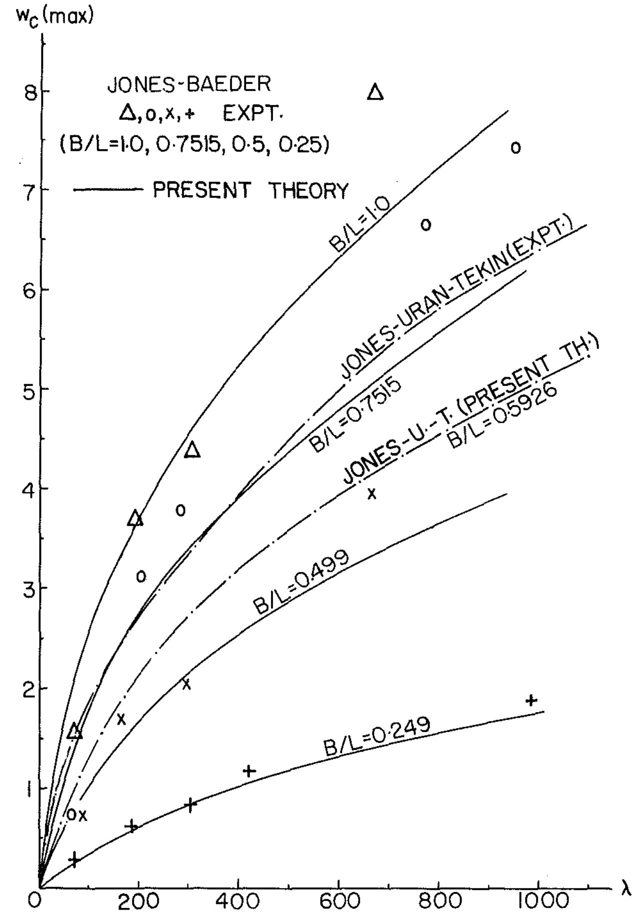

Fig. 3 Maximum permanent deflection versus the nondimensional impulsive load parameter (for mild steel, clamped rectangular plates, Jones-Baeder, 1972, and Jones-Uran-Tekin, 1970)

viscoplastic, clamped rectangular plates with finite deflections, the following two sets of experimental data involving hot-rolled mild steel rectangular plates are chosen as example problems:

(*i*) Jones–Baeder (1972); aspect ratio $B/L = 0.59259$

(*ii*) Jones–Uran–Tekin (1970); aspect ratio $B/L = 0.249$, 0.499, 0.7515, and 1.0

Following Jones (1976), the hinge width to plate thickness ratio varies between 1 and 2 for deflections $w = 0$, $w = 1$, respectively. In the present numerical analysis, the average value of $l/H = 1.5$ is assumed in solving the ordinary differential equation in the small deflection regime ($w_c \le 1.0$). In the large deflection regime ($w_c > 1.0$), the axial stretching is assumed to occur over the entire span so that the hinge width can be approximated by the membrane behavior such that

$$l/H = B/(2H) \quad (50)$$

Further, a sufficiently large value of the dynamic to static pressure ratio is chosen ($\eta = 100$) and this pressure load is essentially equivalent to the impulsive load as predicted by Jones (1971).

Figure 3 shows a graph of the maximum permanent deflection of the center of the mild-steel clamped rectangular plate versus the nondimensional impulsive parameter λ defined by

$$\lambda = \rho V_o{}^2 L^2/M_o \quad (51)$$

where ρ is the mass per unit volume ($\rho = \mu/H$ and for mild-steel, $\rho = 0.00072204$ psi-s^2/in.^{2} or 7.72×10^{-9} N-s^2/mm^4), V_o is the initial velocity, and $M_o = \sigma_o H^2/4$ where σ_o is the yield stress. The aspect ratios of the clamped rectangular plates examined by Jones and Baeder (1972) are $B/L = 0.249$, 0.499,

Table 1 Maximum permanent deflections of mild-steel clamped rectangular plates under impulsive load

Specimen No.	Jones-Baeder Expt.	Jones-Baeder Present Theory	Jones-Uran-Tekin Expt.	Jones-Uran-Tekin Present Theory
1	0.30	0.261	3.542	2.924
2	0.64	0.586	4.120	3.347
3	0.74	0.859	4.650	3.669
4	1.88	1.755	5.166	4.005
5	1.19	0.976	6.420	5.079
6	0.78	0.948	6.730	5.205
7	1.70	1.516	1.046	0.8134
8	2.05	2.108	1.890	1.500
9	3.96	3.299	1.940	1.594
10	0.74	1.468	2.755	2.217
11	3.10	2.741	3.330	2.475
12	3.82	3.385	3.760	2.854
13	6.71	5.425	4.135	3.061
14	7.46	6.069	4.300	3.271
15	1.58	2.044	0.310	0.2089
16	3.69	3.613	0.515	0.3268
17	4.32	4.632	1.022	0.6463
18	7.98	6.593	1.257	0.8300
19	9.31	8.252	1.411	0.9389
20			1.420	0.9334
21			1.580	0.9768
22			1.715	1.042

0.7515, and 1.0; further, $B/L = 0.5926$ refers to Jones–Uran–Tekin (1970) data. Very good correlations between the experimental permanent deflections and the present viscoplastic theoretical results are found for the aspect ratio $B/L = 0.249$ and 0.499 curves. However, for larger aspect ratio $B/L = 0.5926$, 0.7515, and 1.0 and especially for larger values of λ (>300), the present viscoplastic theoretical curves are much lower than the experimental permanent deflections (see Table 1).

The presently derived nonlinear ordinary differential equations for the small and large deflection regime agree exactly with that presented by Jones (1971) for the strain-rate insensitive case ($a=1$, $b=0$) involving aluminum 6061-T6 rectangular plates. Thus, the present theoretical predictions are in good agreement (slightly above) the experimental permanent deflections for all aspect ratios. It should be mentioned that the experimental technique was identical for both the strain-rate insensitive (aluminum) and strain-rate sensitive (mild steel) plates. The theoretical errors due to taking the velocity and displacement fields and the errors due to the neglect of elastic deformations in the energy balance equation are also roughly the same for the strain-rate insensitive and sensitive plates. Assuming that both the errors due to the experiments and those due to the theory do not mutually cancel or are in the same sense, any lack of agreement in the strain-rate sensitive case cannot be attributed to the experimental errors alone (such as in-plane slippage and imperfectly clamped boundary conditions, etc.) or to the above mentioned theoretical assumptions. It is possible that for large aspect ratio and large λ, the strain-rate sensitive behavior of mild steel in "biaxial" states involving plates might not be well approximated by the Cowper–Symonds constitutive relation with coefficients determined by "uniaxial" beam tests. Unfortunately, there is a lack of experimental data for biaxial loadings of strain-rate sensitive materials.

Finally, Tuomala and Mikkola (1980) also predicted substantially lower maximum permanent deflections. They found that the maximum permanent deflections for Jones–Uran–Tekin (1970) specimens No. 9 and 14 are $w_c(\max) = 1.5$ and 3.0 respectively. Using the present viscoplastic theory, one obtains 1.594 and 3.271, respectively; the experimental values are 1.94 and 4.30. Summarizing the results for mild-steel rectangular plates, the present theory is generally in qualitative agreement with the expeirmental data. Thus, the present basic theoretical viscoplastic procedure is acceptable. Further applications of the Cowper–Symonds constitutive equations in collapse of thin-walled tubes (Hui, 1986a) and ice mechanics problems (Hui, 1986b) are in progress.

6 Concluding Remarks

The dynamic plastic behavior of impulsively loaded strain rate sensitive, clamped rectangular plates, incorporating the possibility of finite deflections, has been investigated. Using the Cowper–Symonds constitutive equation, the basic equations were derived and it was found that the dynamic plastic problem can be described by an ordinary differential equation in the small deflection regime and a similar equation in the large deflection range. Based on comparisons with 41 existing experimental data of the maximum permanent deflection of mild steel rectangular plates, it may be concluded that the present theoretical results are in qualitative agreement with the experimental findings. Thus, the present study demonstrates, for the first time, the validity of the energy balance method proposed by Jones (1971) in solving dynamic plastic problems when both strain rate sensitivity and finite deflections are taken into account.

Acknowledgments

Part of the work was done while both authors were associated with the Department of Ocean Engineering, Massachusetts Institute of Technology. Professor Norman Jones (formerly at MIT, now at the University of Liverpool) provided guidance and encouragement throughout the course of this research. The first author would like to acknowledge the partial support from the National Oceanic and Atmospheric Administration (Grant 716576) through the Ohio Sea Grant Program.

References

Ari-Gur, J., Anderson, D. L., and Olson, M. D., (1984), "Review of Air-Blast Response of Beams and Plates," *Proc. of the Second Int. Conf. on Recent Advances in Structural Dynamics*, Univ. of Southampton, April 9-13, 1984, Petyt, M., and Wolfe, H. F., eds., Vol. 1, pp. 383-392.

Hui, D., (1986a), "Design of Beneficial Geometric Imperfections for Collapse of Thin Walled Box Columns under Compression," *Int. J. of Mechanical Sciences*, Vol. 28, No. 3, pp. 163-172.

Hui, D., (1986b), "Viscoelastic Behavior of Floating Ice Plates under Distributed or Concentrated Loads," *Journal of Strain Analysis for Engineering Design*, Vol. 21, No. 3, pp. 135-143.

Hull, T. E., Enright, W. H., and Jackson, K. R., (1976), "User's Guide for DVERK – A Subroutine for Solving Non-Stiff ODE's," University of Toronto, Department of Computer Science, Technical Report No. 100, October p. 36.

Jones, N., Uran, T. O., and Tekin, S. A., (1970), "The Dynamic Plastic Behavior of Fully Clamped Rectangular Plates," *International Journal of Solids and Structures*, Vol. 6, pp. 1499-1512.

Jones, N., (1971), "A Theoretical Study of the Dynamic Plastic Behavior of Beams and Plates With Finite Deflections," *International Journal of Solids and Structures*, Vol. 7, pp. 1007-1029.

Jones, N., and Walters, R. M., (1971), "Large Deflections of Rectangular Plates," *Journal of Ship Research*, Vol. 15, No. 2, June, pp. 164-171.

Jones, N., Griffin, R. N., and Van Duzer, R. E., (1971), "An Experimental Study Into the Dynamic Plastic Behavior of Wide Beams and Rectangular Plates, *International Journal of Mechanical Sciences*, Vol. 13, pp. 721-735.

Jones, N., and Baeder, R. A., (1972), "An Experimental Study of the Dynamic Plastic Behavior of Rectangular Plates," Symposium on Plastic Analysis of Structures, Ministry of Education, Polytechnic Institute of Jassy, Civil Engineering, Rumania, Vol. 1, pp. 476-497; also MIT Ocean Engineering Report No. 72-1.

Jones, N., (1973a), "Slamming Damage," *Journal of Ship Research*, Vol. 17, No. 2, pp. 80-86.

Jones, N., (1973b), "Influence of In-Plane Displacements at the Boundaries of Rigid-Plastic Beams and Plates," *International Journal of Mechanical Sciences*, Vol. 15, pp. 547-561.

Jones, N., (1975), "A Literature Review of the Dynamic Plastic Response of Structures," *The Shock and Vibration Digest*, Vol. 7, No. 8, August, pp. 89-105.

Jones, N., (1976), "Plastic Failure of Ductile Beams Loaded Dynamically," ASME *Journal of Engineering for Industry*, February, pp. 131-136.

Jones, N., (1978a, b, 1981, 1985), "Recent Progress in the Dynamic Plastic Behavior of Structures, Part I," *The Shock and Vibration Digest*, Vol. 10, No. 9, Sept. 1978, pp. 21-33; Part II, Vol. 10, No. 10, Oct. 1978, pp. 13-19; Part III, Vol. 13, No. 10, Oct. 1981, pp. 3-16; Part IV, Vol. 17, No. 2, Feb. 1985, pp. 35-47.

Jones, N., (1979), "Response of Structures to Dynamic Loading," *Proc. of the Second Conf. on the Mechanical Properties of Materials at High Rates of Strain*, Oxford, England, March 28-30, Harding, J., ed., pp. 254-276.

Lee, L. H. N., (1974), "Dynamic Plasticity," *Nuclear Engineering and Design*, Vol. 27, pp. 386-397.

Perrone, N., and Bhadra, P., (1979), "A Simplified Method to Account for Plastic Rate Sensitivity with Large Deformations," ASME JOURNAL OF APPLIED MECHANICS, Vol. 46, pp. 811-816.

Perrone, N., and Bhadra, P., (1984), "Simplified Large Deflection Mode Solutions for Impulsively Loaded, Viscoplastic, Circular Membranes," ASME JOURNAL OF APPLIED MECHANICS, Vol. 51, pp. 505-509.

Sureshwara, B., Lee, L. H. N., and Ariman, T., (1972), "Impulsive Loading of Rectangular Plates With Finite Plastic Deformations," Developments in Theoretical and Applied Mechanics, *Proceedings of the Sixth Southeastern Conf. on Theoretical and Applied Mechanics*, March 23-24, 1972, Henneke E. G., II, and Kranc, S. C., eds., pp. 553-579.

Symonds, P. S., (1965), "Viscoplastic Behavior in Response of Structures to Dynamic Loading," *Behavior of Materials Under Dynamic Loading*, Huffington, N. J., ed., published by ASME, pp. 106-124.

Symonds, P. S., and Jones, N., (1972), "Impulsive Load of Fully Clamped Beams with Finite Plastic Deflections and Strain-Rate Sensitivity," *International Journal of Mechanical Sciences*, Vol. 14, pp. 49-69.

Symonds, P. S., and Wierzbicki, T., (1979), "Membrane Mode Solutions for Impulsively Loaded Circular Plates," ASME JOURNAL OF APPLIED MECHANICS, Vol. 46, No. 1, pp. 58-64.

Symonds, P. S., (1980), "Finite Elastic and Plastic Deformations of Pulse Loaded Structures by an Extended Mode Technique," *International Journal of Mechanical Sciences*, Vol. 22, pp. 597-605.

Taya, M., and Mura, T., (1974), "Dynamic Plastic Behavior of Structures Under Impact Loading Investigated by the Extended Hamilton's Principle," *International Journal of Solids and Structures*, Vol. 10, pp. 197-209.

Tuomala, N. T. E., and Mikkola, M. J., (1980), "Transient Dynamic Large Deflection Analysis of Elastic Viscoplastic Plates by the Finite Element Method," *International Journal of Mechanical Sciences*, Vol. 22, pp. 151-166.

Wojewodzki, W., and Wierzbicki, T., (1972), "Transient Response of Viscoplastic Rectangular Plates," *Archives of Mechanics*, Vol. 24, No. 4, pp. 587-604.

Wojno, W., and Wierzbicki, T., (1979), "On Perturbations Solutions for Impulsively Loaded Viscoplastic Structures," *Journal of Applied Mathematics and Physics* (ZAMP), Vol. 30, pp. 41-55.

Wood, R. H., (1961), *Plastic and Elastic Design of Slabs and Plates*, Thames and Hudson, London.

Wu, R. W. H., (1974), "The Dynamic Plastic Large Deflections of Clamped Rectangular Plate," ASME JOURNAL OF APPLIED MECHANICS, Vol. 41, No. 2, pp. 531-533.

Yankelevsky, D. Z., (1985), "Elasto-Plastic Blast Response of Rectangular Plates," *Int. J. of Impact Engineering*, Vol. 3, No. 2, pp. 107-119.